*The Canadian Mineralogist*
Vol. 42, pp. 545-562 (2004)

# COMPOSITION AND MINERALOGY OF PGE-RICH CHROMITITES IN THE NURALI LHERZOLITE–GABBRO COMPLEX, SOUTHERN URALS, RUSSIA

FEDERICA ZACCARINI[§]

*Department of Earth Sciences, University of Modena and Reggio Emilia, Via S. Eufemia 15, I-41100 Modena, Italy*

EVGENY V. PUSHKAREV AND GERMAN B. FERSHTATER

*Institute of Geology and Geochemistry, Ural Branch, Pochtovy per. 7, 620151 Ekaterinburg, Russia*

GIORGIO GARUTI

*Department of Earth Sciences, University of Modena and Reggio Emilia, Via S. Eufemia 15, I-41100 Modena, Italy*

## ABSTRACT

We have investigated two subeconomic bodies of chromitite in the Nurali lherzolite–gabbro complex, in the southern Urals, Russia, with regard to the composition of the chromian spinel and the distribution and mineralogy of the platinum-group elements (PGE). The bodies of chromitite, referred to as CHR–I and CHR–II, occur as small concordant lenses located at two stratigraphic levels within layered wehrlite and clinopyroxenite, overlying the lherzolitic mantle tectonite. The chromian spinel is Al-rich, showing an increase of Cr/(Cr + Al), $Fe^{2+}/(Fe^{2+} + Mg)$ and $TiO_2$ from CHR–I to CHR–II. The total PGE contents vary from 1.26 to 11.61 ppm, and show increase in (Pt + Pd)/(Os + Ir + Ru) from 0.1 to 52.2 as a result of the appearance of magmatic sulfides in the upper chromitite. The PGM assemblage shows a drastic change from laurite–erlichmanite-dominated to enriched in Pt–Pd sulfides and alloys. Laurite is the first PGM to crystallize, and its composition typically reflects the Ru/Os ratio of the primitive mantle, indicating that the parent melt of the chromitite did not undergo fractionation during ascent. The Nurali chromitites are rather unusual as they have characteristics in common with chromitites associated with ophiolitic cumulates, layered intrusions, Alaskan-type complexes, and the subcontinental orogenic mantle.

*Keywords*: platinum-group minerals, platinum-group elements, chromitites, Nurali complex, Urals, Russia.

## SOMMAIRE

Nous avons étudié deux lentilles sub-économiques de chromitite dans le complexe à lherzolite–gabbro de Nurali, dans la partie sud des Ourales, en Russie, pour en préciser la composition du spinelle chromifère, et la distribution et la minéralogie des éléments du groupe du platine (EGP). Ces lentilles, que l'ont appelle CHR–I et CHR–II, sont petites et concordantes, situées à deux niveaux stratigraphiques dans une séquence stratifiée de wehrlite et de clinopyroxénite qui recouvre la lherzolite mantéllique tectonisée. Le spinelle chromifère fait preuve d'une augmentation en Cr/(Cr + Al), $Fe^{2+}/(Fe^{2+} + Mg)$ et $TiO_2$ en passant de CHR–I à CHR–II. La teneur totale en EGP varie de 1.26 à 11.61 ppm, et il y a augmentation du rapport (Pt + Pd)/(Os + Ir + Ru) de 0.1 à 52.2 comme signe de la présence de sulfures magmatiques dans la chromitite supérieure. L'assemblage de minéraux du groupe du platine change de marquée, d'une dominance de laurite–erlichmanite à une dominance de sulfures de Pt–Pd et d'alliages. La laurite a cristallisé d'abord, et sa composition correspond au rapport Ru:Os du manteau primitif, indication que le magma parent de cette chromitite n'a pas subi de fractionnement lors de sa montée. Les chromitites de Nurali sont plutôt inhabituelles parce qu'elles possèdent des points communs avec les chromitites associées aux cumulats ophiolitiques, aux intrusions stratiformes, aux complexes de type Alaska, et au manteau subcontinental typique des zones orogéniques.

(Traduit par la Rédaction)

*Mots-clés*: minéraux du groupe du platine, éléments du groupe du platine, chromitites, complexe de Nurali, Ourales, Russie.

§ *E-mail address*: fedezac@tsc4.com

## Introduction

The Nurali lherzolite–gabbro complex in the Southern Urals, Russia, consists of mantle tectonite overlain by a dominantly ultramafic layered sequence, passing upward to amphibole gabbro and diorite. Recently, the complex has received different petrological and geotectonic interpretations by scientists working on the Urals. Initially, it was considered as a classic ophiolite sequence characterized by weakly depleted oceanic mantle (Savelieva 1987, Savelieva & Saveliev 1992). More recently, the layered rocks were said to be derived from a source that had undergone substantial depletion at the root of a rift zone (Pertsev *et al.* 1997). However, the ophiolitic affinity of the Nurali complex has been questioned. In fact, the complex is distinct from other ophiolites of the Urals because of the lack of sheeted dykes, pillow lavas and deep-sea sediments. Furthermore, a geochemical study of the Nurali ultramafic–mafic rocks using trace elements, including the rare-earth elements (*REE*) and platinum-group elements (PGE) has revealed some petrological characters consistent with the upper mantle – deep crust transition zone below a continental margin (Fershtater & Bea 1996, Fershtater *et al.* 1997, 1998, Garuti *et al.* 1997a).

In this paper, we investigate subeconomic bodies of chromitite associated with the ultramafic portion of the Nurali layered sequence, and present new data on the composition of the chromian spinel, and the geochemistry and mineralogy of the associated PGE mineralization. Comparisons with geochemical and mineralogical characteristics of other chromitites from different geological settings provide further arguments in the debate concerning the true origin of the Nurali complex.

## Geological and Petrological Background

The Nurali complex is located along the Main Uralian Fault, in the suture zone of the Ural orogenic belt, approximately 30 km south of Miass (Fig. 1). Structural data indicate that the Nurali complex is thrust westward over the Upper Proterozoic metasedimentary units of the Eastern European continental margin during a Paleozoic collision with the Asian plate. Major structural elements of the Nurali rocks (foliation, lithological contacts and layering) are presently tilted into a subvertical position or are steeply inclined eastward, the strike varying from N–S to 30° NNE. Effects of low-grade hydrothermal metamorphism are widespread; the ultramafic rocks have been irregularly serpentinized, and gabbros underwent partial to total rodingitization. Despite of this metasomatic event, primary lithologies are still recognizable.

The mantle tectonite is exposed to the west, in the Nurali Range, and consists of plagioclase–spinel lherzolite, harzburgite and dunite, reaching a total thickness of about 4.5 km. This mantle unit passes eastward into a layered sequence made up of olivine clinopyroxenite, wehrlite, and clinopyroxenite with minor dunite and gabbro. The upper part of the layered sequence consists of a thin horizon of interlayered harzburgite and olivine orthopyroxenite that grades in turn into amphibole-rich melanogabbro, gabbro, diorite and quartz diorite. The total thickness of the cumulate rocks, from the basal contact with residual dunite to the top of the diorite unit, has been estimated to be about 1.5 km. To the east, the Nurali complex is truncated by the serpentinite *mélange* of the Main Uralian Fault, in which large blocks of layered wehrlite–clinopyroxenite and amphibole-rich gabbro and diorite are embedded.

Savelieva (1987) considered the lherzolite – harzburgite – dunite sequence as a typical section through the ophiolitic mantle, resulting from progressive depletion by melt removal in a mid-ocean ridge. Pertsev *et al.* (1997) noted that the ultramafic portion of the layered sequence is similar to the "*transition zone*" that usually separates the mantle tectonite from gabbroic cumulates in an ophiolite complex. These authors proposed that the Nurali transition zone formed by multiple injections of melt derived from a mantle source that was undergoing progressive depletion in a spreading geotectonic setting, at pressures of 6–8 kbar. The common occurrence of amphibole throughout the Nurali transition zone was interpreted as evidence that crystallizing melts were hydrous, although the same authors suggested that these ultramafic cumulate rocks cannot be consanguineous with the overlying amphibole-rich gabbroic rocks, which possibly represent a late intrusive event, not related with the initial ophiolite environment.

Other authors (Fershtater & Bea 1996, Fershtater *et al.* 1997, 1998, Garuti *et al.* 1997a) have provided evidence that the two suites of cumulus rocks apparently have a common geochemical signature with regards to the distribution of trace elements and *REE* and PGE patterns. Thus they are considered to have been emplaced in the same geodynamic environment, not consistent with an ophiolitic oceanic basin. In fact, the amphibole gabbro and diorites have a calc-alkaline affinity, and are remarkably enriched in K and LILE compared with oceanic tholeiites. Similarly, the cumulus clinopyroxenites of the Nurali transition zone have much higher contents of incompatible elements (Sr, Zr, Ba, Ga, Ta, Nb, Hf) and *REE*, and have, on average, higher La/Yb values than the homologous rocks from ophiolite complexes of the Urals (Fershtater *et al.* 1998). At the same time, the depleted mantle-derived rocks display enrichment in some lithophile elements (Rb, Sr, and *LREE*) with respect to mantle restites from most ophiolitic sections of the Urals. According to Fershtater *et al.* (1998), this feature makes the Nurali lherzolite–gabbro complex very similar to orogenic lherzolite massifs from the subcontinental mantle of the Western Alps, Pyrenées, and Betic Cordillera.

The U/Pb isotopic analysis of zircon extracted from a diorite sample from Nurali gave an age of 399 Ma, in

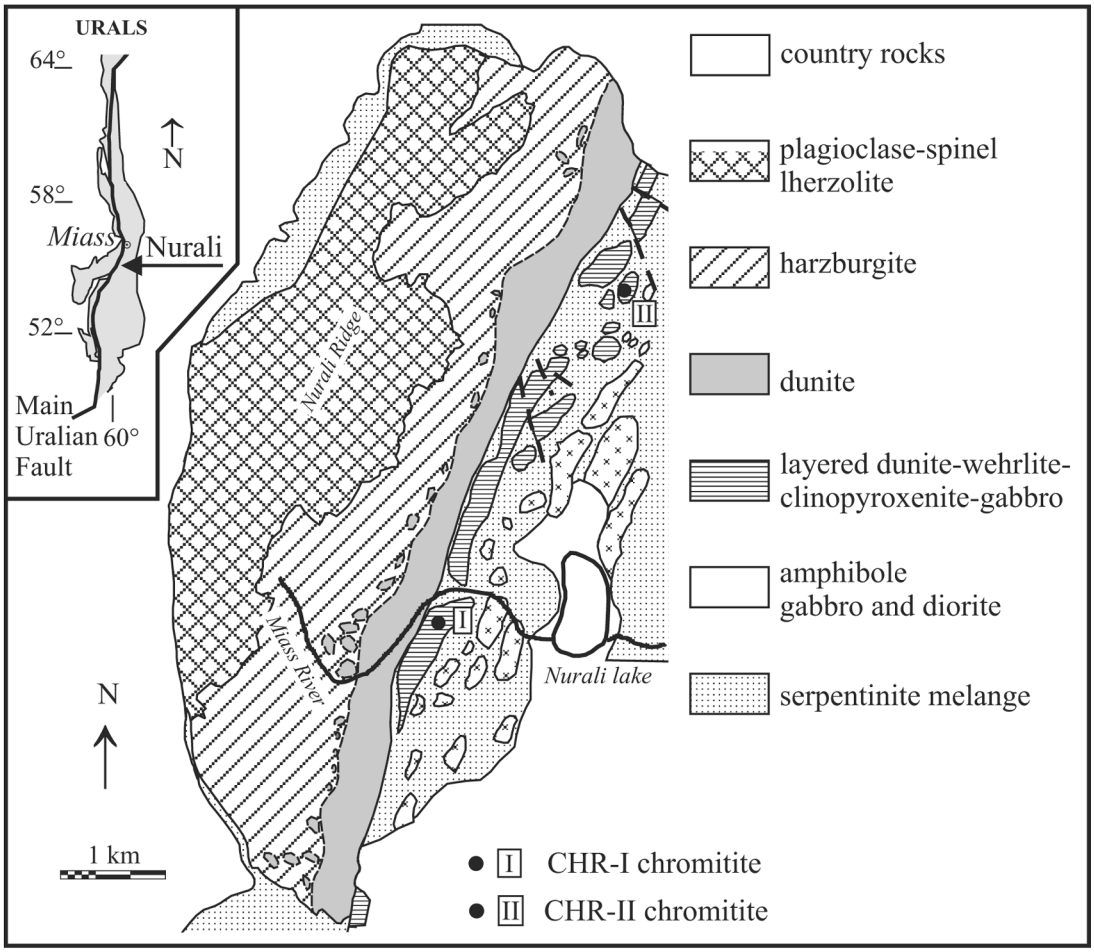


FIG. 1. Geological sketch-map of the Nurali complex, modified after Rudnik (1965), and location of the bodies of chromitite investigated.

agreement with the 390–410 Ma range obtained for most mafic rocks located in the suture zone of the Urals (Fershtater *et al.* 2000). According to those authors, this age corresponds to the pulse of orogenic basic magmatism that is related to the uplift of lherzolite from beneath the passive continental margin to the upper crust during Paleozoic collision between the European and Asian plates.

## ANALYTICAL METHODS

Thirty polished sections cut from 15 samples of chromitite were investigated by optical and electron microscopy and by electron-microprobe analysis. The SEM images were obtained with a Philips XL–40 scanning electron microscope using 20–30 kV accelerating voltage, and 2–10 nA beam current. Analyses were performed using an ARL–SEMQ electron microprobe, operated in the WDS mode, at 15–25 kV accelerating voltage, and 15–20 nA beam current. Compositions of chromian spinel and silicates were obtained by analyzing several grains in each section. Quantitative determinations of Si, Ti, Al, Fe, Mn, Mg, Ca, Cr, Na and K were calibrated on natural minerals: clinopyroxene, olivine, Mn-bearing olivine, albite, microcline, chromite and ilmenite, whereas we used metallic Ni, V, and Zn as standards for the corresponding elements. The proportion of trivalent iron in chromian spinel was calculated assuming stoichiometry. The platinum-group minerals (PGM) were analyzed using pure metals as the reference material for PGE, natural pyrite, chalcopyrite and nickeline for Fe, Ni, Cu, S and As, and synthetic

coloradoite for Hg. The Cr and part of the Fe detected in the analyses of PGM included in chromite are ascribed to spurious fluorescence from direct or secondary excitation of the spinel host.

Total concentrations of the PGE were determined by ICP–MS at the University of Granada (Spain), after the Ni-sulfide-button preconcentration step, carried out at the University of Modena (Italy). The chromitite samples were powdered in an agate mill, and nickel sulfide (stoichiometry $Ni_3S_2$) beads of about 4 grams were obtained by alkaline fusion at 1000°C of 25-gram aliquots of sample. Beads were dissolved in hot concentrated HCl, then PGE were coprecipitated with metallic Te by adding stannous chloride to the solution. The insoluble precipitate was collected on filter paper, then washed to eliminate Ni, and dissolved in warm aqua regia. Spectrometric analysis was performed on the solution obtained after appropriate dilution, and calibrated using the standard UMT–1, certified by CANMET as a reference material. Two additional samples of chromitite were analyzed for PGE and Au by ICP–MS, after Ni-bead pre-concentration and Te coprecipitation, in the Laboratory of the Geological Survey of Finland.

## Chromitites in the Nurali Complex

### *Field relations and petrography*

The occurrence of several subeconomic lenses of chromitite in the Nurali Complex was reported previously by Kravchenko (1986) and, more recently, by Pertsev *et al.* (1997), although no detailed information about precise location, petrography and mineralogy was provided. The chromitites documented here were discovered by S.V. Smirnov in 1990 and were subsequently described by Smirnov & Volchenko (1992) and Moloshag & Smirnov (1996). These lenses of chromitite, which proved to be the largest in the Nurali complex, are found at two distinct localities in the layered ultramafic rocks overlying the mantle unit (Fig. 1). One (CHR–I) occurs in the southern part of the complex, within the wehrlite – clinopyroxenite – dunite – gabbro cumulus sequence, about 150 m above the contact with the dunite unit (Fig. 2A). The chromitite body forms a single elongate lens (10 × 3 m) of massive chromian spinel that extends concordantly with the local layering (strike N–S, dip 60–75°E) and thins out at both ends, grading into minute seams and disseminations. The

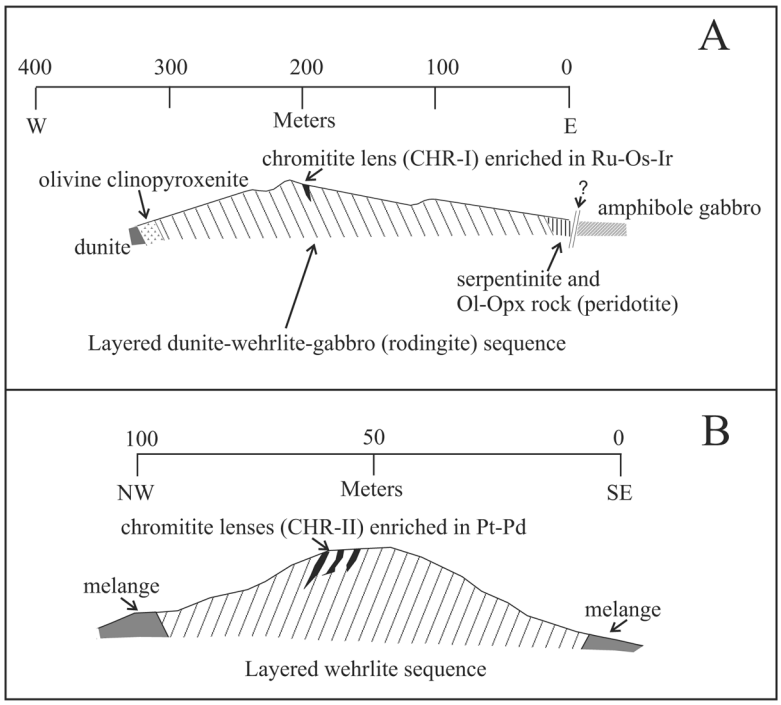


FIG. 2. Geological cross-sections across the chromitite bodies. A) The lower CHR–I chromitite layer is located within interlayered dunite–wehrlite–gabbro, in stratigraphic continuity with the transition-zone dunite. B) The upper CHR–II chromitite occurs inside an isolated block of layered wehrlite, within the tectonic *mélange*.

chromitite is in contact with wehrlite and olivine clinopyroxenite; the occurrence of thin layers of rodingite a few meters below the chromite horizon may possibly mark the first appearance of gabbro from the base of the cumulus sequence.

The other lens of chromitite (CHR–II) is located at the northeastern edge of the Nurali complex, inside a large ultramafic block isolated in the serpentinite *mélange*. The chromitite body consists of the rhythmic repetition of massive seams interlayered with wehrlite and clinopyroxenite, covering an area of about 5 meters wide and more than 30 meters long (Fig. 2B). Massive chromitite grades laterally and along strike into a cloudy dissemination of chromian spinel grains within the clinopyroxenite matrix. The layering in this block is rotated ~45° to the east and dips 60–75°NW, thus the plunge is opposite to that of the pile of cumulates that comprises the CHR–I chromitite layer. However, Fershtater *et al.* (2000) established that in spite of some distortion, the large fragments of layered rocks engulfed in the *mélange* unit are almost undisturbed with respect to their position in the stratigraphy, and they maintain the polarity of the fractionation trend oriented eastward. Therefore, the CHR–II chromitites would seem to lie approximately 150–200 m above the stratigraphic level of CHR–I.

### *Composition and phase relations of the chromian spinel*

At both localities, the chromitite consists of a massive aggregate of spinel (0.3–5.0 mm) with small amounts of silicate gangue (<20 vol.%), mainly consisting of diopside, along with secondary minerals (Cr-rich andradite, grossular, uvarovite and Cr-rich clinochlore). No obvious evidence of gravitational settling was observed. Lobate boundaries, atoll structures, and mutual inclusion relations between chromian spinel and diopside indicate cocrystallization of the two phases. The chromian spinel is variably altered to ferrian chromite along grain boundaries and cracks. As a result, the primary composition of spinel (Table 1) was deduced exclusively from results of the electron-microprobe analysis of grain cores. The relevant variations of major oxides involve increase in total FeO, $Fe_2O_3$ and $TiO_2$ and decrease in MgO, $Al_2O_3$, and $Cr_2O_3$ from CHR–I to CHR–II. Furthermore, the CHR–II spinel has Mn, Zn and V contents higher than CHR–I, but the Ni content is lower. The reciprocal substitutions of Mg–$Fe^{2+}$ and Al–Cr in the tetrahedral and octahedral sites of the spinel structure result in an increase of the values #Cr = Cr/(Cr + Al) and #$Fe^{2+}$ = $Fe^{2+}$/($Fe^{2+}$ + Mg) from the CHR–I to CHR–II, which is consistent with the trend defined by compositions of accessory spinels from the transition zone (Fig. 3).

Systematic differences in the composition of diopside (Table 2) coexisting with chromian spinel have been detected between the two bodies of chromitite. Diopside in the chromitite CHR–I is more magnesian (0.92 < #Mg < 0.98) and has lower Ti, Na, Al, and Cr contents than diopside in CHR–II (0.86 < #Mg < 0.90). The more strongly magnesian diopside in CHR–I is accompanied by orthopyroxene, minor pargasite and accessory phlogopite. Olivine was not encountered; we believe, however, that it must have been an important component of the original assemblage on account of the abundant serpentine and magnetite, in part pseudomorphic, in the samples. In CHR–II, diopside is the only primary silicate and shows remarkable levels of Al, Ti, Na and Cr, up to values of 2.8 wt% $Al_2O_3$, 0.18% $TiO_2$, 0.28% $Na_2O$ and 0.85% $Cr_2O_3$, respectively. Accessory titanium minerals (titanite, ilmenite, and rutile) are commonly found associated with the interstitial matrix of the chromitite. Furthermore, it is noteworthy that the CHR–II contains relatively abundant base-metal sulfides (BMS). Pyrrhotite, pentlandite, millerite and minor chalcopyrite generally occur as inclusions in chromite, and may form composite inclusions with PGM, whereas heazlewoodite, Cu-rich alloy, awaruite and wairauite are found disseminated in the altered sili-

TABLE 1. REPRESENTATIVE COMPOSITION OF CHROMIAN SPINEL FROM THE NURALI CHROMITITES

| | CHR-I | | | | | CHR-II | | | | |
|---|---|---|---|---|---|---|---|---|---|---|
| | NU 9A | NU 44 | NU 46 | NU 49 | NU 50A | NU 65B | NU 66A | NU 66 | NU 67 | NU 68 |
| $SiO_2$ wt% | 0.16 | 0.02 | 0.06 | 0.03 | 0.00 | 0.08 | 0.04 | 0.10 | 0.16 | 0.00 |
| $TiO_2$ | 0.08 | 0.05 | 0.07 | 0.06 | 0.04 | 0.69 | 0.82 | 0.85 | 0.79 | 0.76 |
| $Al_2O_3$ | 26.25 | 30.63 | 27.33 | 31.27 | 28.15 | 20.53 | 19.28 | 19.21 | 18.10 | 20.63 |
| FeO | 12.64 | 12.43 | 10.56 | 9.01 | 13.59 | 21.90 | 21.14 | 20.32 | 20.33 | 21.18 |
| $Fe_2O_3$ | 3.76 | 3.95 | 6.18 | 7.56 | 4.47 | 14.98 | 14.19 | 15.50 | 14.82 | 14.79 |
| MnO | 0.21 | 0.09 | 0.19 | 0.24 | 0.24 | 0.30 | 0.33 | 0.29 | 0.32 | 0.35 |
| MgO | 15.11 | 15.66 | 16.22 | 17.72 | 14.40 | 8.61 | 9.06 | 9.52 | 9.53 | 9.18 |
| $Cr_2O_3$ | 40.59 | 36.08 | 37.33 | 32.86 | 37.17 | 32.07 | 34.04 | 32.90 | 34.97 | 32.50 |
| NiO | 0.32 | 0.27 | 0.21 | 0.32 | 0.32 | 0.19 | 0.11 | 0.17 | 0.14 | 0.09 |
| ZnO | 0.01 | 0.04 | 0.09 | 0.02 | 0.02 | 0.19 | 0.25 | 0.20 | 0.21 | 0.27 |
| $V_2O_3$ | 0.17 | 0.18 | 0.14 | 0.10 | 0.14 | 0.27 | 0.35 | 0.24 | 0.43 | 0.35 |
| Total | 99.30 | 99.39 | 98.47 | 99.21 | 98.54 | 99.81 | 99.62 | 99.31 | 99.81 | 100.10 |
| Si *apfu* | 0.00 | 0.00 | 0.00 | 0.00 | 0.00 | 0.00 | 0.00 | 0.00 | 0.01 | 0.00 |
| Ti | 0.00 | 0.00 | 0.00 | 0.00 | 0.00 | 0.02 | 0.02 | 0.02 | 0.02 | 0.02 |
| Al | 0.93 | 1.07 | 0.97 | 1.07 | 1.00 | 0.78 | 0.74 | 0.73 | 0.69 | 0.78 |
| $Fe^{2+}$ | 0.32 | 0.31 | 0.27 | 0.22 | 0.34 | 0.59 | 0.57 | 0.55 | 0.55 | 0.57 |
| $Fe^{3+}$ | 0.09 | 0.09 | 0.14 | 0.17 | 0.10 | 0.36 | 0.35 | 0.38 | 0.36 | 0.36 |
| Mn | 0.01 | 0.00 | 0.00 | 0.01 | 0.01 | 0.01 | 0.01 | 0.01 | 0.01 | 0.01 |
| Mg | 0.68 | 0.69 | 0.73 | 0.77 | 0.65 | 0.41 | 0.44 | 0.46 | 0.46 | 0.44 |
| Cr | 0.97 | 0.84 | 0.89 | 0.76 | 0.89 | 0.82 | 0.87 | 0.84 | 0.90 | 0.82 |
| Ni | 0.01 | 0.01 | 0.01 | 0.01 | 0.01 | 0.01 | 0.00 | 0.00 | 0.00 | 0.00 |
| Zn | 0.00 | 0.00 | 0.00 | 0.00 | 0.00 | 0.00 | 0.01 | 0.00 | 0.00 | 0.01 |
| V | 0.00 | 0.00 | 0.00 | 0.00 | 0.00 | 0.00 | 0.00 | 0.00 | 0.01 | 0.00 |
| #Cr | 0.51 | 0.44 | 0.48 | 0.41 | 0.47 | 0.51 | 0.54 | 0.53 | 0.56 | 0.51 |
| #$Fe^{2+}$ | 0.32 | 0.31 | 0.27 | 0.22 | 0.35 | 0.59 | 0.57 | 0.55 | 0.54 | 0.56 |
| #$Fe^{3+}$ | 0.04 | 0.04 | 0.07 | 0.08 | 0.05 | 0.19 | 0.18 | 0.19 | 0.19 | 0.18 |

The stoichiometry of the spinel is calculated on the basis of four oxygen atoms; *apfu*: atoms per formula unit. #Cr = Cr/(Cr + Al), #$Fe^{2+}$ = $Fe^{2+}$/($Fe^{2+}$ + Mg), #$Fe^{3+}$ = $Fe^{3+}$/($Fe^{3+}$ + Cr + Al).

cate matrix, in some cases associated with secondary PGM.

## PGE Mineralization in the Nurali Chromitites

### *PGE abundance in chromitite and enclosing rocks*

The Nurali chromitites are rich in noble metals (Table 3), with overall PGE concentrations of 1.26 ppm and 11.61 ppm, and Au contents varying from 2 to 14 ppb. Chondrite-normalized patterns of distribution are presented in Figure 4, and compared with those obtained for layered rocks in the Nurali complex (Garuti *et al.* 1997a). The distribution patterns of the two chromitites display pronounced fractionation of the PGE, emphasized by an increase of the (Pt + Pd)/(Os + Ir + Ru) value from 0.01 in the lower chromitite to 52.2 in the upper one. Mafic and ultramafic layered rocks contain a hundred to a thousand times lower ΣPGE than the chromitites (Table 3) and show a decrease in ΣPGE content from wehrlites to gabbros. Notably, one sample of wehrlite from the ultramafic cumulates below CHR–I has a rather flat PGE pattern, with (Pt + Pd)/(Os + Ir + Ru) as low as 1.7. The slope of the PGE pattern becomes positive in wehrlite samples above CHR–I, with (Pt + Pd)/(Os + Ir + Ru) increasing up to 10.6–12.5. Gabbroic cumulates from above the CHR–II chromitite are characterized by a deep negative anomaly in Pt, with Pd and Au as the dominant noble metals. Thus the variation of the PGE patterns of enclosing rocks is consistent with that of the chromitites, showing fractionation of the refractory Os–Ir–Ru (*i.e.,* the IPGE) from the low-melting Rh–Pt–Pd (*i.e.,* the PPGE), similar to that resulting from magmatic differentiation processes.

### *The platinum-group minerals*

More than 400 PGM grains from 2 to 35 μm in size were located in polished sections, with a frequency of

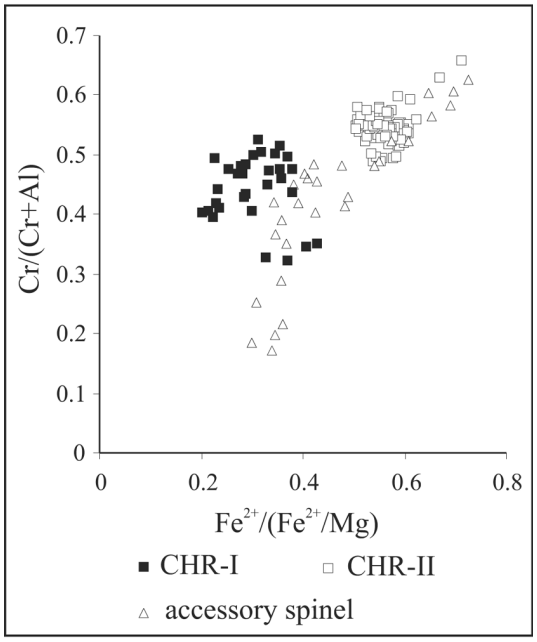


FIG. 3. Compositional variations of chromian spinel from the CHR–I and CHR–II chromitites (present work) and accessory chromian spinel from the ultramafic layered rocks of the Nurali complex (Pertsev *et al.* 1997, and unpublished data of the authors).

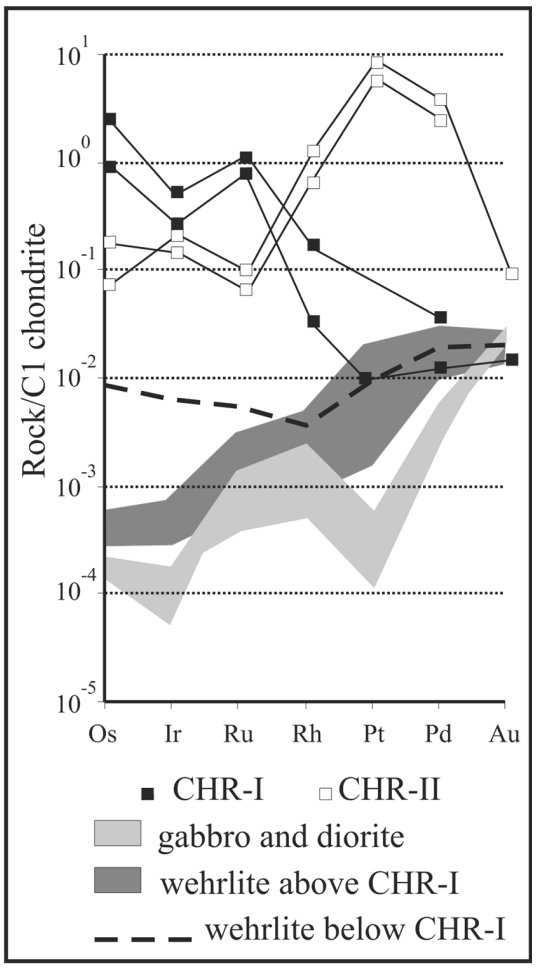


FIG. 4. Chondrite-normalized PGE patterns compared with distribution patterns for wehrlite below CHR–I, wehrlite above CHR–I, and gabbro above CHR–II. Source of data for unmineralized rocks: Garuti *et al.* (1997a). Chondrite-normalization values from Naldrett & Duke (1980).

TABLE 2. REPRESENTATIVE COMPOSITIONS OF CLINOPYROXENE FROM THE NURALI CHROMITITES

| | CHR-I | | | CHR-II | | | | | | | | |
|---|---|---|---|---|---|---|---|---|---|---|---|---|
| | NU 9A 1 | NU 9A 2 | NU 9A 3 | NU 65A1 | NU 66A 1 | NU 66A 2 | NU 67 1 | NU 67 3 | NU 67 4 | NU 68 1 | NU 68 2 | NU 68 4 |
| $SiO_2$ wt% | 54.01 | 54.33 | 54.43 | 53.80 | 53.11 | 53.39 | 53.23 | 52.63 | 53.58 | 53.03 | 52.84 | 53.15 |
| $TiO_2$ | 0.02 | 0.03 | 0.04 | 0.11 | 0.13 | 0.13 | 0.13 | 0.15 | 0.14 | 0.14 | 0.16 | 0.13 |
| $Al_2O_3$ | 1.44 | 1.63 | 1.36 | 1.45 | 2.02 | 2.00 | 1.92 | 1.86 | 1.46 | 1.89 | 2.15 | 1.93 |
| FeO | 1.54 | 1.34 | 0.83 | 3.29 | 3.72 | 3.71 | 3.70 | 3.45 | 3.71 | 3.85 | 3.52 | 4.05 |
| MnO | 0.06 | 0.00 | 0.11 | 0.12 | 0.13 | 0.12 | 0.14 | 0.06 | 0.14 | 0.15 | 0.11 | 0.11 |
| MgO | 18.39 | 18.01 | 20.79 | 17.22 | 16.66 | 17.15 | 16.97 | 17.22 | 17.56 | 16.70 | 17.77 | 17.42 |
| CaO | 23.75 | 22.07 | 21.43 | 22.99 | 22.25 | 22.31 | 22.69 | 22.85 | 22.58 | 22.32 | 22.49 | 22.13 |
| $Na_2O$ | 0.00 | 0.16 | 0.14 | 0.21 | 0.26 | 0.20 | 0.22 | 0.25 | 0.20 | 0.22 | 0.20 | 0.22 |
| $K_2O$ | 0.00 | 0.06 | 0.05 | 0.00 | 0.00 | 0.00 | 0.01 | 0.02 | 0.00 | 0.00 | 0.00 | 0.00 |
| $Cr_2O_3$ | 0.23 | 0.43 | 0.39 | 0.56 | 0.53 | 0.75 | 0.57 | 0.53 | 0.45 | 0.82 | 0.58 | 0.60 |
| NiO | 0.00 | 0.00 | 0.00 | 0.00 | 0.00 | 0.00 | 0.00 | 0.00 | 0.07 | 0.00 | 0.12 | 0.06 |
| Total | 99.45 | 98.05 | 99.56 | 99.74 | 98.80 | 99.77 | 99.57 | 99.03 | 99.70 | 99.12 | 99.92 | 99.81 |
| Si *apfu* | 1.96 | 1.99 | 1.96 | 1.96 | 1.96 | 1.95 | 1.95 | 1.94 | 1.96 | 1.95 | 1.93 | 1.94 |
| Ti | 0.00 | 0.00 | 0.00 | 0.00 | 0.00 | 0.00 | 0.00 | 0.00 | 0.00 | 0.00 | 0.00 | 0.00 |
| $^{IV}Al$ | 0.04 | 0.01 | 0.05 | 0.04 | 0.04 | 0.05 | 0.05 | 0.08 | 0.04 | 0.05 | 0.09 | 0.06 |
| $^{VI}Al$ | 0.02 | 0.06 | 0.01 | 0.03 | 0.05 | 0.04 | 0.03 | 0.01 | 0.02 | 0.04 | 0.00 | 0.02 |
| Fe | 0.05 | 0.04 | 0.03 | 0.10 | 0.11 | 0.11 | 0.11 | 0.11 | 0.11 | 0.12 | 0.11 | 0.12 |
| Mn | 0.00 | 0.00 | 0.00 | 0.00 | 0.00 | 0.00 | 0.00 | 0.00 | 0.00 | 0.00 | 0.00 | 0.00 |
| Mg | 1.00 | 0.98 | 1.12 | 0.94 | 0.92 | 0.93 | 0.93 | 0.95 | 0.96 | 0.92 | 0.97 | 0.95 |
| Ca | 0.92 | 0.87 | 0.83 | 0.90 | 0.88 | 0.87 | 0.89 | 0.90 | 0.88 | 0.88 | 0.88 | 0.87 |
| Na | 0.00 | 0.01 | 0.01 | 0.01 | 0.02 | 0.01 | 0.02 | 0.02 | 0.01 | 0.02 | 0.01 | 0.02 |
| K | 0.00 | 0.00 | 0.00 | 0.00 | 0.00 | 0.00 | 0.00 | 0.00 | 0.00 | 0.00 | 0.00 | 0.00 |
| Cr | 0.01 | 0.01 | 0.01 | 0.02 | 0.02 | 0.02 | 0.02 | 0.02 | 0.01 | 0.02 | 0.02 | 0.02 |
| Ni | 0.00 | 0.00 | 0.00 | 0.00 | 0.00 | 0.00 | 0.00 | 0.00 | 0.00 | 0.00 | 0.01 | 0.00 |
| #Mg | 0.96 | 0.96 | 0.98 | 0.90 | 0.89 | 0.89 | 0.89 | 0.90 | 0.89 | 0.89 | 0.90 | 0.88 |
| #Cr | 0.22 | 0.17 | 0.61 | 0.38 | 0.24 | 0.37 | 0.35 | 0.75 | 0.39 | 0.40 | 0.87 | 0.48 |

The stoichiometry of the clinopyroxene is calculated on the basis of six oxygen atoms. #Mg = Mg/(Mg + Fe), #Cr = Cr/(Cr + $^{VI}Al$).

one to seven grains per square centimeter of explored surface. On the basis of both textural and paragenetic evidence, two generations of PGM can be distinguished: 1) Primary PGM, formed in the high-temperature magmatic stage before, during, and after the precipitation of chromite: sulfides of the laurite–erlichmanite series, accompanied by minor Os–Ir–Ru alloy, rhodian pentlandite and rare kashinite in CHR–I, and Pt–Fe alloy and PGE sulfides such as laurite, erlichmanite and cooperite in CHR–II. 2) Secondary PGM, formed at a relatively low temperature, during some postmagmatic event: Ru–Os–Ir–Fe oxide in CHR–I and Pt–Pd–Fe–Cu–Ni alloy, potarite and Pt–Pd-bearing awaruite and wairauite in CHR–II.

These results are fully consistent with the geochemical data, and confirm preliminary observations by Moloshag & Smirnov (1996) that the chromitites contain distinct populations of PGM, CHR–I dominated by Ru–Os–Ir minerals, and CHR–II having much higher proportions of Pt–Pd phases relative to Ru–Os–Ir minerals.

TABLE 3. CONCENTRATIONS (ppb) OF NOBLE METALS IN THE NURALI CHROMITITES AND CUMULUS WEHRLITE AND GABBRO

| | CHR -Ia | CHR -Ib | CHR -IIa | CHR -IIb | Wh 1 | Wh 2 | Wh 3 | Wh 4 | Gb 1 | Gb 2 | Gb 3 | Gb 4 |
|---|---|---|---|---|---|---|---|---|---|---|---|---|
| Os | 1286 | 473 | 97 | 40 | 4.41 | 0.15 | 0.31 | 0.11 | 0.14 | 0.07 | 0.12 | 0.12 |
| Ir | 278 | 154 | 80 | 111 | 3.48 | 0.21 | 0.43 | 0.05 | 0.16 | 0.03 | 0.09 | 0.06 |
| Ru | 746 | 605 | 42 | 62 | 3.74 | 0.68 | 2.21 | 0.95 | 0.41 | 0.75 | 0.27 | 0.38 |
| Rh | 36 | 7.02 | 130 | 263 | 0.73 | 0.29 | 1.03 | 0.49 | 0.16 | 0.39 | 0.11 | 0.18 |
| Pt | n.d. | 10.90 | 5997 | 8940 | 9.55 | 4.11 | 20.69 | 0.45 | 1.70 | 0.60 | 0.12 | 0.58 |
| Pd | 19 | 6.68 | 1396 | 2190 | 10.25 | 6.94 | 16.12 | 2.24 | 4.94 | 2.43 | 1.41 | 3.19 |
| Au | n.d. | 2.24 | n.d. | 14 | 3.05 | 2.16 | 4.29 | 3.32 | 3.75 | 4.17 | 4.36 | 3.98 |
| Pd/Ir | 0.07 | 0.04 | 17.50 | 19.73 | 2.94 | 33.19 | 37.67 | 45.00 | 30.88 | 81.00 | 15.67 | 53.17 |
| (Pt + Pd)/(Os + Ir + Ru) | | 0.01 | 33.82 | 52.23 | 1.70 | 10.60 | 12.48 | 2.43 | 9.36 | 3.56 | 3.20 | 6.75 |

Data for CHR-Ib and CHR-IIb were obtained from the Geological Survey of Finland. Wehrlite (Wh) and Gabbro (Gb) data are from Garuti *et al.* (1997a). Wh 1: wehrlite below the CHR-I layer, Wh 2–4 : wehrlite above the CHR-I layer.

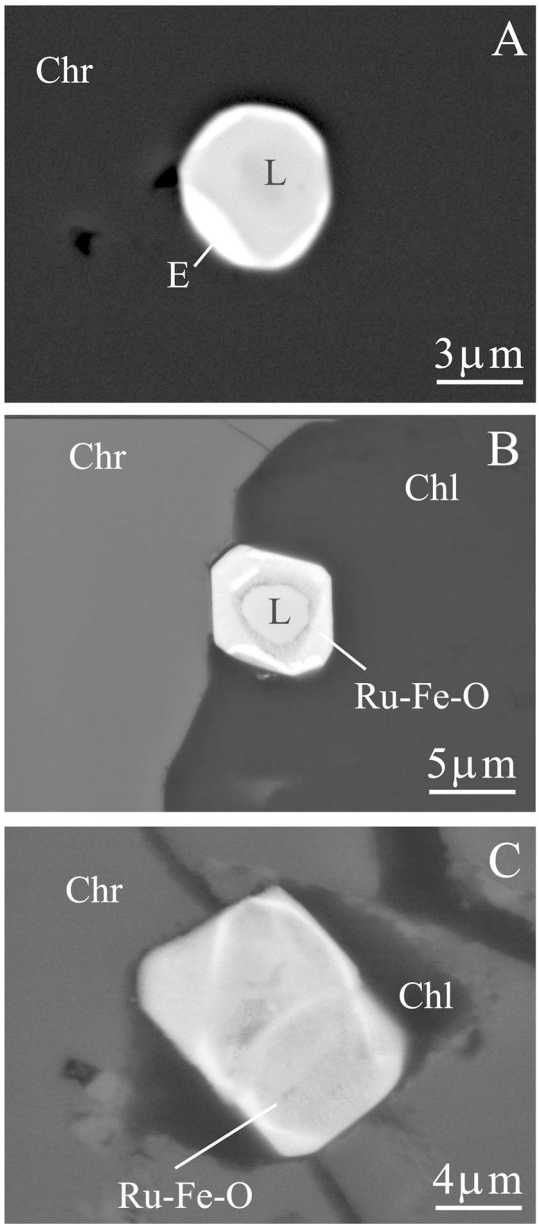


FIG. 5. BSE images of Ru–Os–Ir minerals associated with the CHR–I chromitite of Nurali. A) Primary grain of laurite (L) with erlichmanite (E) rim included in fresh chromite (Chr). B) *In situ* altered grain of laurite (L) replaced by oxide (Ru–Fe–O) and metallic Os (white), at the boundary between chromite (Chr) and chlorite (Chl). C) Ru–Fe oxide in contact with chlorite (Chl) and altered chromite (Chr).

Laurite is the most abundant PGM in CHR–I and usually occurs included in fresh chromite, in some cases associated with clinopyroxene, pargasite, and millerite. Compositions (Table 4) exhibit enrichment in Ir up to 2.08 at.% and, in some cases, in Rh and Pd, up to 0.24 and 0.67 at.%, respectively. Compositional zoning was detected in some cases, with an increase in Os at the rim of laurite leading to erlichmanite (Fig. 5A), although the opposite pattern also exists. The osmium alloy contains from 4 to 21 at.% Ir. The secondary Ru–Os–Ir–Fe and Os–Ru–Ir–Fe oxides were described for the first time by Garuti *et al.* (1997b), who suggested a possible origin by low-temperature desulfuration and further oxidation of pre-existing crystals of laurite and erlichmanite. Conclusive support of this assumption is brought by the discovery of a number of zoned grains composed of a laurite core rimmed by oxide (Fig. 5B). The observed process of alteration of laurite and erlichmanite involves progressive loss of S and gain of Fe and O, apparently without change in volume since the external shape of the original sulfide crystal is generally preserved (Fig. 5C).

The Pt–Pd rich assemblage in the CHR–II chromitite consists of primary Pt–Fe alloy and rare cooperite, along with secondary Pt–Pd–Fe–Cu–Ni alloy, potarite (Table 4) and (Pt,Pd)-bearing Ni–Fe–Co alloys, possibly awaruite and wairauite. Minerals pertaining to the laurite–erlichmanite series also are present, but they are much less abundant than in CHR–I and contain less Ir. The grains of primary Pt–Fe alloy are less than 10 μm across, and occur exclusively included in unaltered chromite as part of composite aggregates with pyrrhotite (Figs. 6A, B). Compositions of the Pt–Fe alloy are consistent with tetraferroplatinum-type stoichiometry (PtFe), although a precise classification is hampered by the lack of X-ray-diffraction data. The grains of secondary Pt–Pd–Fe–Cu–Ni alloy have a wide range of composition and cannot be unambiguously ascribed to any known phase. The secondary PGM are systematically found in the altered silicate matrix or along cracks cutting across chromite crystals, typically associated with garnet and chromian clinochlore (Figs. 6C, D, E, F). Because of these textural relations, we believe that they formed by reaction with hydrothermal fluids, involving both *in situ* alteration of primary PGM and direct deposition of PGE from hydrous solutions. In contrast with the primary PGM included in chromian spinel, the assemblage of secondary PGM contains abundant Pd and Cu (Figs. 6C, E, F). We do not believe that these metals were added to the chromitites from an external source during hydrothermal alteration. On the contrary, paragenetic observations suggest that they were derived by the alteration of an intercumulus PGE-rich sulfide phase, originally located interstitially to the grains of chromian spinel. The presence of abundant grains of primary sulfides still preserved as inclusions in fresh chromian spinel, as well as of relics of sulfides in the altered matrix (Figs. 6C, D), supports this assumption.

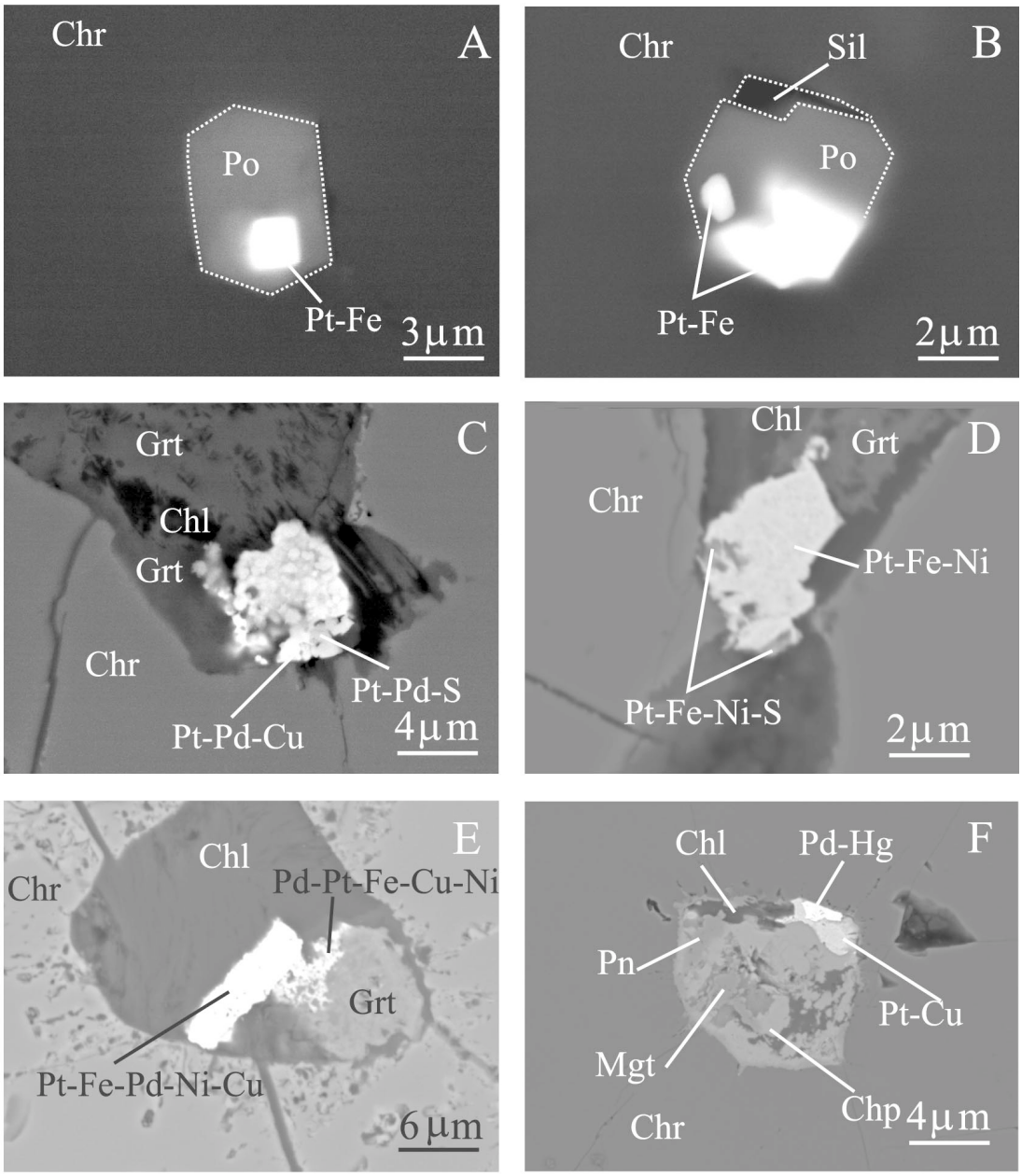


FIG. 6. BSE images of Pt and Pd minerals associated with the CHR–II chromitite of Nurali. A) Composite inclusion of pyrrhotite (Po) and Pt–Fe alloy in unaltered chromite. B) Grain composed of pyrrhotite (Po), Pt–Fe alloy and silicate (Sil) in fresh chromite. C) Secondary alloy of Pt–Pd–Cu and Pt–Pd sulfide associated with garnet (Grt) and chlorite (Chl) in altered chromite (Chr). D) Secondary alloy of Pt–Fe–Ni and Pt–Fe–Ni sulfide associated with garnet (Grt) and chlorite (Chl) in altered chromite (Chr). E) Secondary alloys of Pt–Pd and base metals associated with garnet (Grt) and chlorite (Chl) in altered chromite (Chr). F) Composite grain in altered chromite (Chr): potarite (Pd–Hg), Pt–Cu alloy, pentlandite (Pn), chalcopyrite (Chp), magnetite (Mgt) and chlorite (Chl).

TABLE 4. SELECTED MICROPROBE COMPOSITIONS OF LAURITE, Pt ALLOYS AND POTARITE FROM THE NURALI CHROMITITES

| Weight % | Os | Ir | Ru | Rh | Pt | Pd | Ni | Fe | Cu | S | As | Hg | Tot. |
|---|---|---|---|---|---|---|---|---|---|---|---|---|---|
| Laurite-erlichmanite from CHR-I | | | | | | | | | | | | | |
| NU44 14 1 | 28.17 | 5.86 | 33.36 | 0.38 | 0.21 | 0.88 | 0.56 | 0.77 | 0.00 | 32.73 | 0.00 | n.a. | 102.91 |
| NU44 23c 1 | 24.23 | 5.43 | 36.53 | 0.00 | 0.20 | 1.06 | 0.01 | 0.00 | 0.00 | 30.59 | 0.00 | n.a. | 98.06 |
| NU44 26 1 | 28.30 | 6.15 | 33.08 | 0.00 | 0.00 | 1.05 | 0.45 | 0.64 | 0.00 | 32.22 | 0.00 | n.a. | 101.87 |
| NU44 2a 1 | 23.26 | 5.16 | 37.32 | 0.00 | 0.38 | 1.03 | 0.32 | 0.30 | 0.00 | 30.96 | 0.00 | n.a. | 98.74 |
| NU45 16 1 | 26.46 | 3.69 | 35.26 | 0.33 | 0.00 | 0.15 | 0.02 | 0.75 | 0.00 | 32.85 | 0.00 | n.a. | 99.51 |
| NU43 3 core | 12.89 | 0.48 | 52.92 | 0.20 | 0.00 | 0.45 | 0.00 | 0.00 | 0.02 | 35.01 | 0.00 | n.a. | 101.95 |
| NU43 3 rim | 45.51 | 0.00 | 28.48 | 0.11 | 0.00 | 0.19 | 0.00 | 0.00 | 0.00 | 28.66 | 0.00 | n.a. | 102.95 |
| NU46 2 core | 55.64 | 1.27 | 11.21 | 0.05 | 0.00 | 0.18 | 0.37 | 0.38 | 0.00 | 27.47 | 0.00 | n.a. | 96.57 |
| NU46 2 rim | 46.39 | 2.78 | 17.75 | 0.15 | 0.00 | 0.19 | 0.35 | 0.26 | 0.00 | 29.11 | 0.00 | n.a. | 96.98 |
| NU46 3 core | 14.15 | 2.14 | 48.19 | 0.00 | 0.00 | 0.48 | 0.26 | 0.24 | 0.00 | 36.37 | 0.00 | n.a. | 101.82 |
| NU46 3 rim | 71.03 | 0.00 | 3.10 | 0.00 | 0.00 | 0.08 | 1.04 | 0.39 | 0.00 | 25.91 | 0.94 | n.a. | 102.49 |
| Primary Pt-Fe alloys from CHR-II | | | | | | | | | | | | | |
| NU65b 8 1 | 0.03 | 0.00 | 0.00 | 0.35 | 68.99 | 3.89 | 0.64 | 22.30 | 0.12 | 0.35 | 0.06 | n.a. | 96.73 |
| NU65b 8 3 | 0.22 | 0.00 | 0.01 | 0.49 | 76.01 | 3.46 | 0.15 | 14.20 | 0.70 | 0.62 | 0.13 | n.a. | 95.99 |
| NU65b 10 1 | 0.06 | 0.00 | 0.02 | 0.69 | 72.67 | 3.82 | 0.15 | 22.47 | 0.00 | 0.45 | 0.00 | n.a. | 100.33 |
| NU65b 10 2 | 0.00 | 0.00 | 0.06 | 0.59 | 75.51 | 3.61 | 0.26 | 18.72 | 0.00 | 0.40 | 0.22 | n.a. | 99.35 |
| Secondary Pt-Pd-Fe-Cu alloys from CHR-II | | | | | | | | | | | | | |
| NU65b 7 2 | 0.11 | 0.00 | 0.00 | 0.46 | 56.62 | 1.74 | 0.53 | 26.23 | 12.74 | 0.56 | 0.32 | n.a. | 99.31 |
| NU65b 9 5 | 0.13 | 0.00 | 0.00 | 0.78 | 58.08 | 14.26 | 0.47 | 14.01 | 10.14 | 0.42 | 0.08 | n.a. | 98.37 |
| NU65b 9 6 | 0.00 | 0.00 | 0.00 | 0.26 | 10.61 | 28.42 | 0.01 | 2.42 | 56.11 | 0.22 | 0.00 | n.a. | 98.05 |
| NU65b 9 8 | 0.00 | 0.00 | 0.00 | 0.50 | 10.16 | 26.22 | 0.00 | 6.44 | 53.62 | 0.77 | 0.00 | n.a. | 97.71 |
| Secondary Potarite from CHR-II | | | | | | | | | | | | | |
| NU65A 3b 1 | n.a. | n.a. | n.a. | n.a. | n.a. | 33.19 | 0.058 | 0.852 | 0.037 | 0.133 | n.a. | 65.39 | 99.66 |
| NU65A 3b 2 | n.a. | n.a. | n.a. | n.a. | n.a. | 32.53 | 0.072 | 1.012 | 0.77 | 0.131 | n.a. | 65.61 | 100.12 |

| Atomic % | Os | Ir | Ru | Rh | Pt | Pd | Ni | Fe | Cu | S | As | Hg | Ru/Os |
|---|---|---|---|---|---|---|---|---|---|---|---|---|---|
| Laurite-erlichmanite from CHR-I | | | | | | | | | | | | | |
| NU44 14 1 | 9.46 | 1.95 | 21.08 | 0.24 | 0.07 | 0.53 | 0.61 | 0.88 | 0.00 | 65.20 | 0.00 | n.a. | 2.23 |
| NU44 23c 1 | 8.59 | 1.91 | 24.38 | 0.00 | 0.07 | 0.67 | 0.01 | 0.00 | 0.00 | 64.37 | 0.00 | n.a. | 2.84 |
| NU44 26 1 | 9.65 | 2.08 | 21.23 | 0.00 | 0.00 | 0.64 | 0.49 | 0.74 | 0.00 | 65.18 | 0.00 | n.a. | 2.20 |
| NU44 2a 1 | 8.12 | 1.78 | 24.51 | 0.00 | 0.13 | 0.64 | 0.36 | 0.35 | 0.00 | 64.10 | 0.00 | n.a. | 3.02 |
| NU45 16 1 | 8.97 | 1.24 | 22.50 | 0.20 | 0.00 | 0.09 | 0.02 | 0.87 | 0.00 | 66.10 | 0.00 | n.a. | 2.51 |
| NU43 3 core | 4.00 | 0.15 | 30.94 | 0.11 | 0.00 | 0.25 | 0.00 | 0.00 | 0.01 | 64.53 | 0.00 | n.a. | 7.73 |
| NU43 3 rim | 16.87 | 0.00 | 19.87 | 0.07 | 0.00 | 0.13 | 0.00 | 0.00 | 0.00 | 63.06 | 0.00 | n.a. | 1.18 |
| NU46 2 core | 22.81 | 0.51 | 8.65 | 0.04 | 0.00 | 0.13 | 0.49 | 0.53 | 0.00 | 66.83 | 0.00 | n.a. | 0.38 |
| NU46 2 rim | 17.99 | 1.07 | 12.95 | 0.10 | 0.00 | 0.13 | 0.44 | 0.35 | 0.00 | 66.96 | 0.00 | n.a. | 0.72 |
| NU46 3 core | 4.35 | 0.65 | 27.88 | 0.00 | 0.00 | 0.26 | 0.26 | 0.25 | 0.00 | 66.34 | 0.00 | n.a. | 6.41 |
| NU46 3 rim | 29.87 | 0.00 | 2.46 | 0.00 | 0.00 | 0.06 | 1.42 | 0.56 | 0.00 | 64.64 | 1.00 | n.a. | 0.08 |
| Primary Pt-Fe alloys from CHR-II | | | | | | | | | | | | | Pt/Fe |
| NU65b 8 1 | 0.02 | 0.00 | 0.00 | 0.41 | 43.26 | 4.47 | 1.34 | 48.84 | 0.24 | 1.32 | 0.09 | n.a. | 0.95 |
| NU65b 8 3 | 0.16 | 0.00 | 0.01 | 0.67 | 54.34 | 4.54 | 0.35 | 35.47 | 1.53 | 2.68 | 0.25 | n.a. | 1.58 |
| NU65b 10 1 | 0.04 | 0.00 | 0.03 | 0.80 | 44.64 | 4.30 | 0.31 | 48.21 | 0.00 | 1.66 | 0.00 | n.a. | 1.01 |
| NU65b 10 2 | 0.00 | 0.00 | 0.07 | 0.73 | 49.48 | 4.34 | 0.58 | 42.86 | 0.00 | 1.58 | 0.37 | n.a. | 1.24 |
| Secondary Pt-Pd-Fe-Cu alloys from CHR-II | | | | | | | | | | | | | PGE/BM |
| NU65b 7 2 | 0.06 | 0.00 | 0.00 | 0.45 | 28.66 | 1.62 | 0.89 | 46.39 | 19.81 | 1.71 | 0.42 | n.a. | 0.46 |
| NU65b 9 5 | 0.08 | 0.00 | 0.00 | 0.87 | 34.11 | 15.36 | 0.91 | 28.74 | 18.29 | 1.51 | 0.13 | n.a. | 1.05 |
| NU65b 9 6 | 0.00 | 0.00 | 0.00 | 0.20 | 4.32 | 21.24 | 0.01 | 3.44 | 70.23 | 0.55 | 0.00 | n.a. | 0.35 |
| NU65b 9 8 | 0.00 | 0.00 | 0.00 | 0.38 | 4.05 | 19.16 | 0.00 | 8.96 | 65.59 | 1.87 | 0.00 | n.a. | 0.32 |
| Secondary Potarite from CHR-II | | | | | | | | | | | | | |
| NU65A 3b 1 | n.a. | n.a. | n.a. | n.a. | n.a. | 47.34 | 0.15 | 2.32 | 0.09 | 0.63 | n.a. | 49.47 | |
| NU65A 3b 2 | n.a. | n.a. | n.a. | n.a. | n.a. | 45.75 | 0.18 | 2.71 | 1.81 | 0.61 | n.a. | 48.93 | |

## Sulfur Fugacity in the Nurali Chromitites

The mineral assemblages of primary PGM inclusions in the Nurali chromitites can be modeled as a function of temperature, T, and sulfur fugacity, $f(S_2)$ (Fig. 7). Laurite can crystallize directly from basaltic melts at temperature as high as 1250–1300°C and sulfur fugacities in terms of log $f(S_2)$ comprised between –2 and –1.3 (Brenan & Andrews 2001), thus well below the sulfide-saturation threshold for mafic silicate melts. These values probably correspond to the initial T–$f(S_2)$ conditions in the lower chromitite layer (CHR–I), and trended toward higher $f(S_2)$ with decreasing T during precipitation of chromian spinel, although they never exceeded the stability of erlichmanite. The appearance of pyrrhotite + cooperite and pyrrhotite + Pt–Fe alloy assemblages in CHR–II implies a relatively high fugacity of sulfur in the parent melt. Formation of a true immiscible sulfide liquid in the pre-chromite stage is unlikely, since the occurrence of laurite in the assemblage, although as a minor component, indicates that $f(S_2)$ was initially below the value required for sulfide saturation (Merkle 1992). However, the abundance of BMS and the Cu–Pd-rich nature of the PGM occurring interstitially to chromian spinel support the hypothesis that sulfide saturation was certainly achieved in the late stage of chromite crystallization, leading to a high (Pt + Pd)/(Os + Ir + Ru) value in the CHR–II chromitite.

## Comparison with Chromitite from Various Geological Settings

### *Composition of the chromian spinel*

The composition of chromian spinel from the Nurali chromitites is compared with the compositional fields of chromitites from different geological settings in Figures 8 and 9. The compositional fields portrayed refer to massive chromite ores and do not include compositions of disseminated spinel from mafic and ultramafic rocks.

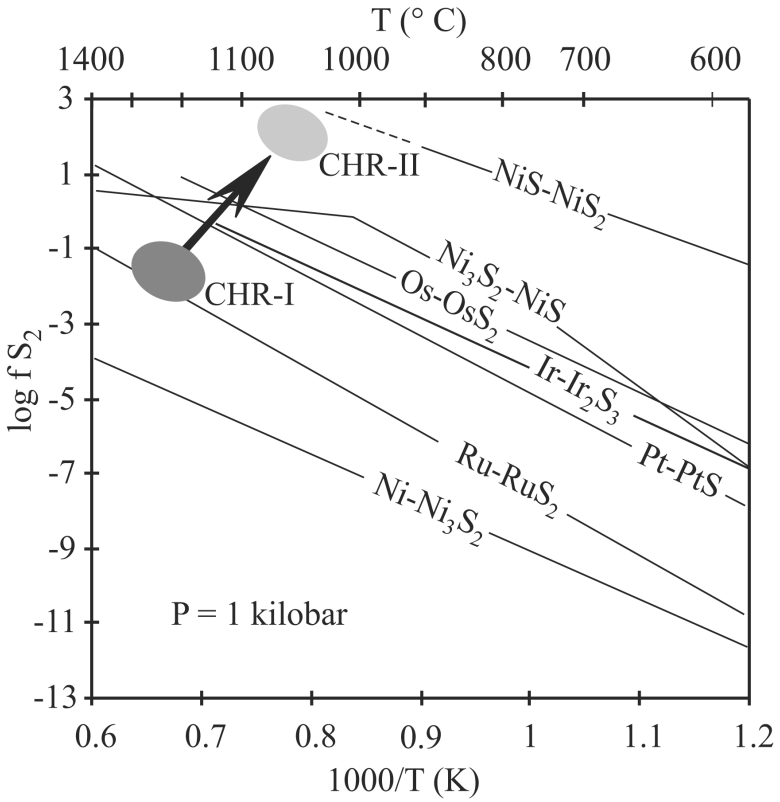


FIG. 7. Metal–sulfide equilibrium curves for Ru, Pt, Os, Ir, and Ni as function of sulfur fugacity [expressed as log $f(S_2)$] and temperature (T), modified after Garuti *et al.* (1999b). The hypothetical fields of CHR–I and CHR–II and the fractionation trend (arrow) are shown.

The Nurali chromitites, as a whole, definitely differ from high-Cr, low-Ti podiform chromitites hosted in the mantle section of ophiolites of the Urals (Garuti *et al.* 1999b, c, Melcher *et al.* 1999) and analogous chromitites from China (Zhou & Bai 1992) in which the composition of the spinel matches that crystallized from boninitic basalts (Roeder 1994) in suprasubduction zones. Because of its low #Cr, the CHR–I somewhat resembles the Al-rich podiform chromitites from the upper-mantle sections or the supra-Moho cumulates of ophiolites, which are believed to have been derived from tholeiitic basalts formed in mid-oceanic-ridge (MORB), ocean-island (OIB) or island arc (IAT) settings. However, the CHR–I displays remarkable differences, having higher Al compared with the Al-rich chromitites from New Caledonia (Augé & Maurizot 1995), Kempirsai (Economou-Eliopoulos & Zhelyaskova-Panayotova 1998, Melcher *et al.* 1997, 1999), eastern Cuba (Proenza *et al.* 1999) and Othrys (Fig. 9). The CHR–II is definitely different from ophiolitic chromitites in general for its enrichment in Ti, and higher $\#Fe^{2+}$ and $\#Fe^{3+}$ numbers (Figs. 8, 9). The Nurali chromitites are enriched in Al compared with chromitites in layered intrusions and Alaskan-type complexes, and notably display $\#Cr$–$\#Fe^{2+}$ relationships opposite to the differentiation trends of both types, characterized by a decrease of #Cr with increasing $\#Fe^{2+}$ (Stowe 1994, Garuti *et al.* 2003). In this respect, the Nurali chromitites bear some similarity to a small group of subeconomic chromitites located in the lherzolite massifs of the Betic Cordillera (southern Spain and northern Morocco), namely the "Cr-ores" and the "Cr–Ni-ores" of Gervilla & Leblanc (1990) and Leblanc *et al.* (1990), which are believed to have crystallized from magmas migrating from the core area to the margins of subcontinental mantle diapirs, during uplift into the crust. However, even in this case, there are remarkable differences concerning the extent of the compositional variations (Fig. 8).

*PGE patterns*

The PGE pattern of the CHR–I chromitite has a negative slope typical of mantle-hosted chromitites of ophiolite complexes. In contrast, the slope of the CHR–II pattern is remarkably positive, similar to that of the PGE-sulfide reefs. Therefore the Nurali chromitites differ from the Al-rich chromitites in ophiolitic cumulates of the Urals (Fig. 10) and others of Chinese orogenic belts (not shown in the figure), which are characterized by very low contents of PGE and by chondrite-normalized patterns varying from nearly flat to moderately positive (Melcher *et al.* 1997, Zhou *et al.* 1998). A positive slope similar to that of the CHR–II chromitite has been reported from cumulus chromitites in some ophiolite complexes, such as, for example, New Caledonia, Zambales, Thetford Mines, and Albania (Augé & Maurizot 1995, Bacuta *et al.* 1987, Burgath 1999, Gauthier *et al.* 1990). However, unlike Nurali, the PPGE enrichment in these ophiolites occurs in passing from the chromitites inside the mantle section to those located above the mantle–crust transition (Moho surface).

The Nurali chromitites display a variation of the PGE pattern from negative to positive similar to that reported from stratiform chromitites of the Bushveld complex, passing from the Lower to the Upper Group of layers (Naldrett & Von Gruenewaldt 1989), or that of chromitites of the Betic Cordillera, in passing from the core (Cr-ores) to the periphery (Cr–Ni-ores) of the subcontinental mantle diapir (Leblanc *et al.* 1990). In all these examples, as in the case of Nurali, the decoupling of IPGE from PPGE occurs as a result of early fractionation of Os–Ir–Ru and generation of residual liquids enriched in Rh–Pt–Pd, which are removed from the magma at a subsequent stage by segregation of a S(+As) melt.

*The role of laurite as a petrogenetic indicator*

Laurite is the most common PGM in chromitites from various geotectonic settings. In most occurrences, it is recognized as a pristine liquidus phase that becomes included in chromian spinel soon after crystallization. Its composition thus is a potential indicator of the initial conditions of temperature, sulfur fugacity and relative activities of Ru and Os in the parent melt (Augé & Johan 1988). Compositions of laurite from layered intrusions (Bushveld, Stillwater, Bird River sill), ophiolite complexes (Ray–Iz, Kempirsai, Kraka, Kluchevskoy, Vourinos, Othrys, Skyros, Rhodope, Bulqiza, Tropoya, Troodos, Guleman, Samail, Acoje, Tiebaghi, Massif du Sud, Luobusa-Donqiao, Meratus–Bobaris, Thetford Mines) and the subcontinental mantle of the Betic Cordillera (Ojén) are compared with those from Nurali in terms of the system Ru–Os–(Ir + Rh) (Fig. 11).

According with the database reported by Garuti *et al.* (1999a, b), most chromitites from the suboceanic mantle typically contain laurite and Os–Ru–Ir alloy occurring as discrete inclusions within the grains of chromian spinel. The alloys crystallize before laurite (Augé & Johan 1988), removing Os preferentially from the melt; thereby, the composition of laurite is forced to be enriched in Ru with respect to the chondritic atomic ratio ($Ru_{72}Os_{28}$). This assemblage formed at low $f(S_2)$, straddling the Ru–$RuS_2$ reaction line over a relatively narrow range of about two log units. The fact that in Figure 11 the compositional field of laurite from ophiolitic suites has been depicted as covering the entire range of Ru–Os substitution is due to compositions from a few chromite deposits (Tiebaghi, Kempirsai, Ray–Iz), in which $f(S_2)$ increased more than four log units across the Ru–$RuS_2$ buffer. In these suites, discrete grains of Os-rich laurite and erlichmanite, as well as a variety of Ir–Rh sulfides, occur associated with inclusions of laurite and Os–Ru–Ir alloy, among other

PGM, in the chromian spinel. For those occurrences, the crystallization of chromian spinel may have been shifted down to a relatively low temperature, possibly due to a high activity of fluid in the parent melt of the chromitites (Melcher *et al.* 1999, Garuti *et al.* 1999b), and $f(S_2)$ had the opportunity to increase up to values that are unusual for the chromite-forming systems within ophiolitic mantle.

The compositions of laurite from stratiform chromitites of layered intrusions cluster in a very narrow field close to the Ru apex, suggesting that $f(S_2)$ was well below saturation in the pre-chromite stage (Merkle 1992), and possibly reflecting a non-chondritic Ru/Os value in the parent melt that may depend on Os fractionation before emplacement or the mechanism of partial melting, or even a non-chondritic Ru/Os value at the source.

In contrast with chromitites from the suboceanic mantle, the "Cr-ores" in the subcontinental mantle of the Betic Cordillera are characterized by the absence of an Os–Ir–Ru alloy, indicating that $f(S_2)$ was initially above the Ru–$RuS_2$ buffer, and they contain a complex assemblage of Ir–Rh–Pt sulfides (Garuti *et al.* 1995, Torres-Ruiz *et al.* 1996), which suggests that $f(S_2)$ was high at the pre-chromite stage. Laurite was the first PGM to crystallize, and compositions show dense clus-

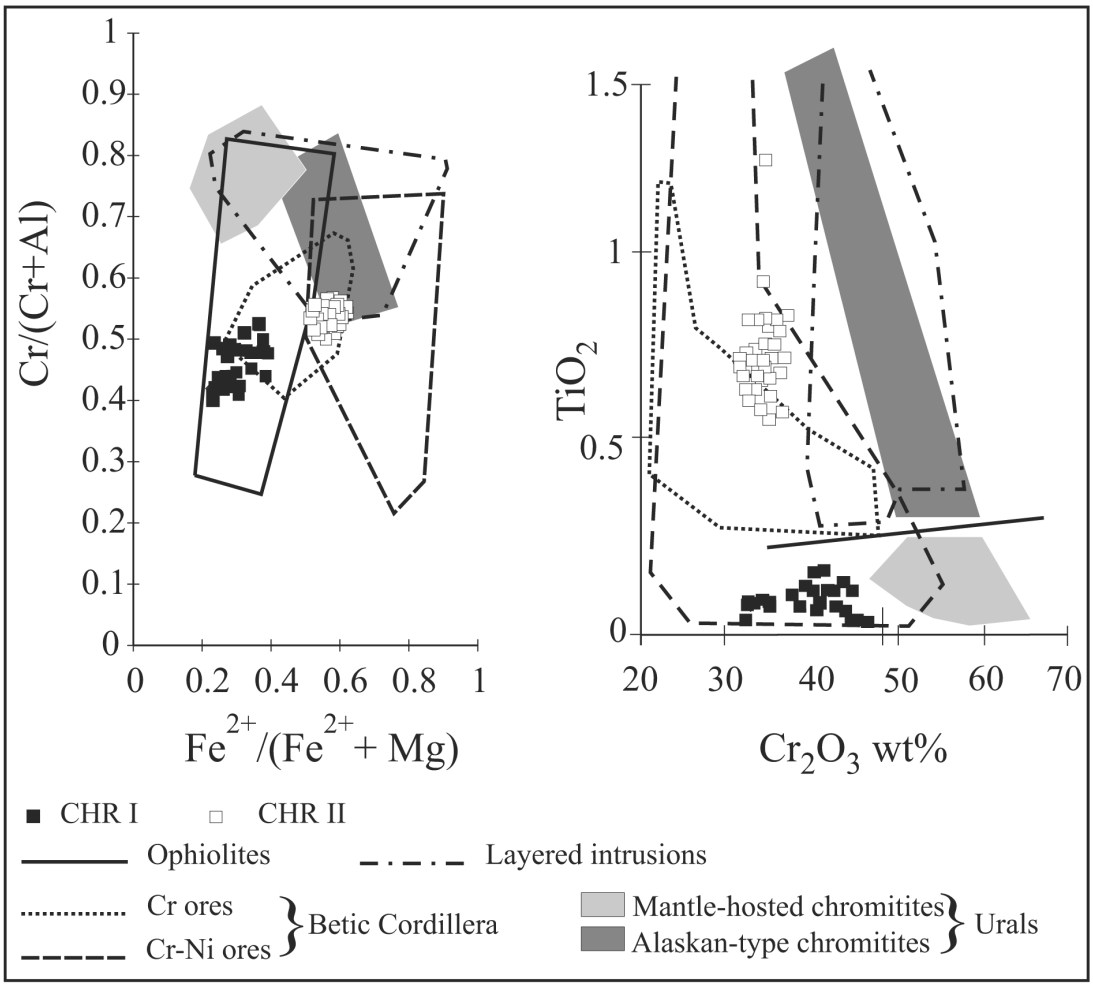


FIG. 8. Compositional variations of chromite from massive chromitite in different geotectonic settings. Dark gray field: chromitites in Alaskan-type complexes of the Urals (Tagil, Kachkanar, Kytlym, Uktus); light-gray field: chromitites in ophiolitic mantle tectonites of the Urals (Kempirsai, Ray–Iz, Kluchevskoy, Kraka). Source of data: unpublished original data of the authors plus others from Economou-Eliopoulos (1996), Garuti *et al.* (1999a, b, c, 2003), Gervilla & Leblanc (1990), Leblanc & Nicolas (1992), Mussallam *et al.* (1981), Melcher *et al.* (1999), Ohnenstetter *et al.* (1986), Zhou & Bai (1992).

tering close to the chondritic ratio ($Ru_{72}Os_{28}$), a feature that has been observed exclusively in the Al-rich chromitites of Othrys (Greece) and is absent in the Mesozoic and Paleozoic ophiolite complexes worldwide (Garuti *et al.* 1999a, b). The observed compositional zoning in laurite grains from the Nurali chromitites (Figs. 5A, 11) may be due to fluctuation of thermodynamic parameters [T–$f(S_2)$] during fractionation; however, if the strongly zoned grains displaying in turn high Ru/Os or Os/Ru values are excluded, the laurite grains have a Ru:Os proportion close to being chondritic, similar to that of laurite from the subcontinental mantle at Ojén. Important implications are that i) in contrast with initial conditions prevailing in the ophiolitic environment, chromitites at Nurali and Ojén formed under initially high $f(S_2)$, and ii) their parent melts were "unfractionated" with respect to the Ru:Os ratio in the primitive mantle, in contrast to what is the case for the melts parent to stratiform chromitites in continental layered intrusions of the Bushveld type.

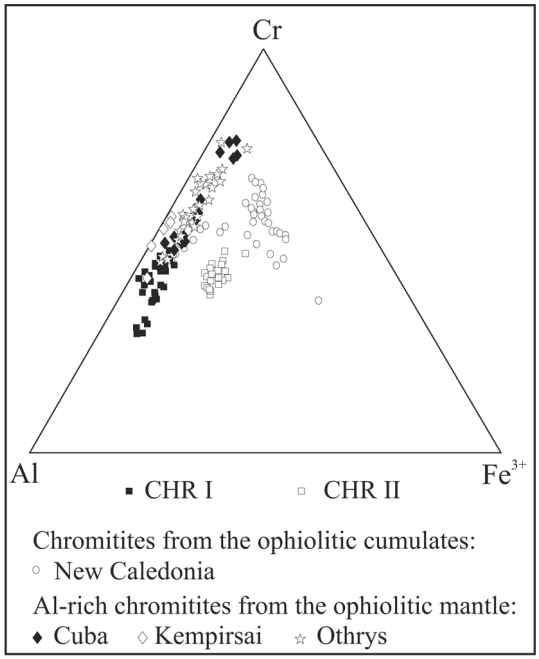


FIG. 9. Comparison of composition of chromite from the Nurali chromitites (CHR–I and CHR–II) with those of the ophiolitic cumulates from New Caledonia (Augé & Maurizot 1995), and Al-rich chromitites from Cuba (Proenza *et al.* 1999), Kempirsai (Melcher *et al.* 1999, Economou-Eliopoulos & Zhelyaskova-Panaytova 1998) and Othrys (unpublished original data of the authors).

## CONCLUSIONS

1) Although the occurrence of the Nurali chromitites in two separate blocks prevents us from ascertaining their true stratigraphic distance, both field evidence and petrological data unequivocally indicate that the CHR–II group of layers was originally located above the CHR–I chromitite lens. Pertsev *et al.* (1997) suggested that the ultramafic layered sequence hosting the chromitites formed by multistage intrusion and fractionation of hydrous magmas ponding above a dominantly lherzolitic mantle tectonite. Compositional variation of the chromian spinel from CHR–I to CHR–II, and its relations with the coexisting clinopyroxene are interpreted as effects of the same mechanism of intrusion and fractionation that generated the sequence of layered rocks.

2) At Nurali, the chromitites are the main concentrator of PGE; they contain up to thousand times higher ΣPGE than the associated silicate rocks. The PGE contents are as high as in the PGE-rich chromitites of the Bushveld Complex, and are determined by the accumulation of abundant crystals of laurite inside the chromian spinel in the lower layer (CHR–I), and preferential concentration of Pd–Pt PGM interstitial to chromian spinel in the upper one (CHR–II). The trend of PGE fractionation and the results of the mineralogical study suggest that at Nurali, the precipitation of chromian spinel occurred at relatively high $f(S_2)$ compared with ophiolitic chromitites, although sulfide saturation was attained only in the latest stage of crystallization of the upper chromitite layer.

3) The composition of the chromian spinel and the distribution and mineralogy of the PGE allow some speculation concerning the possible composition of the parent melt. The composition of the chromian spinel in CHR–I suggests that the parent magma was relatively rich in Al, compared with magmas parent to chromitites hosted in the mantle section of ophiolites. At the same time, the more differentiated chromitite, CHR–II, has $\#Fe^{2+}$ and $\#Fe^{3+}$ values and a Ti content much higher than those expected for high-Al chromitites crystallized from MORB-type basalts. The inclusions of primary laurite in the lower chromitite layer are characterized by Ru and Os in chondritic proportions, which distinguishes the Nurali chromitites from those in most ophiolite complexes and Bushveld-type layered intrusions. Both the chondritic composition of laurite, on one hand, and the complementary shapes of the PGE patterns, on the other, strongly suggest that the parent melt of the chromitites was unfractionated with regards to its PGE content.

4) In view of the contrasting models proposed for the tectonic setting of the Nurali complex, the results of this study do not lead to a conclusive answer, but they provide further argument for debate. The Nurali chromitites are quite unusual compared with those commonly occurring in ophiolites. At the same time, they

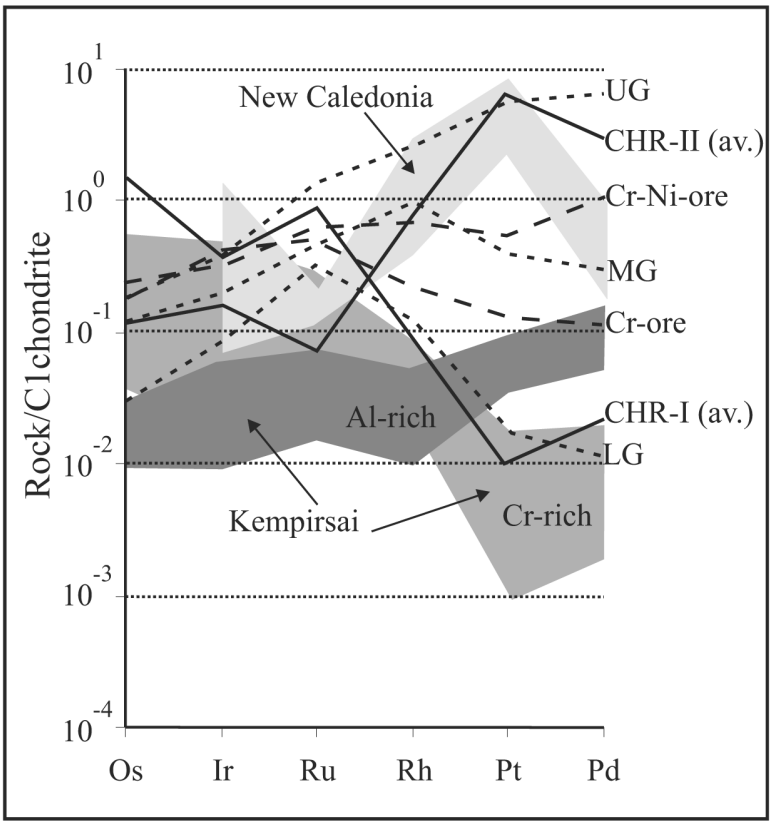


FIG. 10. Comparison of PGE chondrite-normalized patterns for the Nurali chromitites (CHR–I and CHR–II) with those of the high-Cr and high-Al chromitites from Kempirsai (Melcher *et al.* 1999), the cumulates-hosted chromitite from New Caledonia (Augé & Maurizot 1995), the Lower Group (LG), Middle Group (MG) and Upper Group (UG) chromitites from the Bushveld Complex (Cawthorn 1999), and the "Cr-ore" and "Cr–Ni-ore" from the Betic Cordillera (Leblanc *et al.* 1990, Gervilla & Leblanc 1990).

do not conform consistently with the characters of chromitites from other geological settings, such as layered intrusions, Alaskan-type complexes, or the subcontinental orogenic mantle. We note, however, that the Nurali chromitites appear to have been derived from magmas characterized by a relatively high Al:Cr ratio, a primitive (*i.e.,* unfractionated) PGE composition, and initially a high $f(S_2)$, which suggest an origin by partial melting of a fertile source. These features would appear to be more consistent with an undepleted subcontinental mantle than the depleted mantle beneath the oceans.

## ACKNOWLEDGEMENTS

The Italian Ministero della Università e della Ricerca Scientifica e Tecnologica is thanked for the financial support of this investigation (COFIN 2002). We are grateful to T. Augé and S. Arai for their critical comments, and to J. Mungall and R.F. Martin for their editorial reviews, which have substantially contributed to improve the paper.

## REFERENCES

AUGÉ, T. & JOHAN, Z. (1988): Comparative study of chromite deposits from Troodos, Vourinos, North Oman and New Caledonia ophiolites. *In* Mineral Deposits within the European Community (J. Boissonnas & P. Omenetto, eds.). Springer, Berlin, Germany (267-288).

_____ & MAURIZOT, P. (1995): Stratiform and alluvial platinum mineralization in the New Caledonian ophiolite complex. *Can. Mineral.* **33**, 1023-1045.

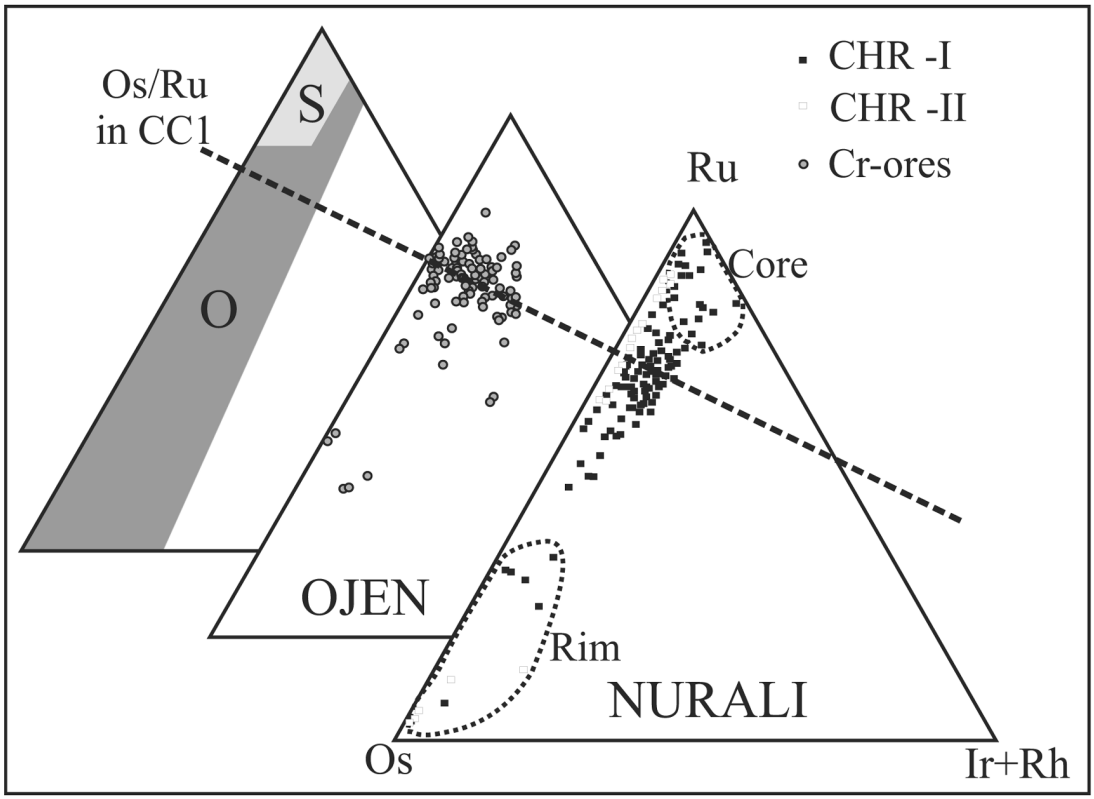


FIG. 11. Compositions of PGM of the laurite–erlichmanite series included in chromite of the Nurali chromitites. The dashed fields include core-to-rim compositions from zoned grains, the straight dashed line marks the Ru/Os atomic ratio in the CC1 chondrite. Ojén: compositions of laurite–erlichmanite PGM included in the "Cr-ores" (Torres-Ruiz *et al.* 1996). (S): field of laurite inclusions in stratiform chromitite from the layered intrusions of Bushveld, Stillwater and Bird River Sill (Maier *et al.* 1999, Ohnenstetter *et al.* 1986, Talkington & Lipin 1986, Zaccarini *et al.* 2002). (O): field of laurite–erlichmanite PGM inclusions in mantle-hosted chromitites from various ophiolite complexes (Garuti *et al.* 1999a, b, c).

BACUTA, G.C., LIPIN, B.R., GIBBS, A.K. & KAY, R.W. (1987): Platinum-group element abundance in chromitite deposits of the Acoje ophiolite block, Zambales ophiolite complex, Philippines. *In* Geoplatinum 87 (H.M. Prichard *et al.*, eds.). Elsevier Applied Sciences, London, U.K. (381-382).

BRENAN, J.M. & ANDREWS, D. (2001): High-temperature stability of laurite and Ru–Os–Ir alloy and their role in PGE fractionation in mafic magmas. *Can. Mineral.* **39**, 341-360.

BURGATH, P.K. (1999): Der Albanische Miridte Ophiolit und sene PGE Anreicherungen. *Mitt. Osterr. Mineral. Ges.* **144**, 23-44.

CAWTHORN, R.G. (1999): Geological models for platinum-group metal mineralization in the Bushveld Complex. *S. Afr. J. Sci.* **95**, 490-498.

ECONOMOU-ELIOPOULOS, M. (1996): Platinum-group element distribution in chromite ores from ophiolite complexes: implications for their exploration. *Ore Geol. Rev.* **11**, 363-381.

_____ & ZHELYASKOVA-PANAYTOVA, M. (1998): Comparative study of the geochemistry of chromite ores from the Kempirsai (Urals) and Rhodope (Balkan Peninsula) ophiolitic massifs. *Bull. Geol. Soc. Greece* **32**(3), 203-211.

FERSHTATER, G.B. & BEA, F. (1996): Geochemical classification of ophiolites from the Urals. *Geokhim.* **3**, 195-218 (in Russ.).

_____, _____, BORODINA, N.S. & MONTERO, P. (1998): Lateral zonation, evolution, and geodynamic interpretation of magmatism of the Urals: new petrological and geochemical data. *Petrology* **6**(5), 409-433.

_____, KOTOV, A.B., SMIRNOV, S.V., PUSHKAREV, E.V., SAL'NIKOVA, E.B., KOVACK, V.P., YOKOVLEVA, S.Z. & BEREZHNAYA, N.G. (2000): U–Pb zircon age of diorite from the Nurali lherzolite–gabbro massif in the Southern Urals. *Dokl. Earth Sci.* **371**, 365-368.

_____, MONTERO, P., BORODINA, N. S., PUSHKAREV, E.V., SMIRNOV, S.V. & BEA, F. (1997): Uralian magmatism: an overview. *Tectonophys*. **276**, 87-102.

GARUTI, G., FERSHTATER, G.B., BEA, F., MONTERO, P., PUSHKAREV, E.V. & ZACCARINI, F. (1997a): Platinum-group elements as petrological indicators in mafic-ultramafic complexes of the central and southern Urals: preliminary results. *Tectonophys*. **276**, 181-194.

_____, GAZZOTTI, M. & TORRES-RUIZ, J. (1995): Iridium, rhodium and platinum sulfides in chromitites from the ultramafic massifs of Finero, Italy, and Ojén, Spain. *Can. Mineral*. **33**, 509-520.

_____, PUSHKAREV, E.V., ZACCARINI, F., CABELLA, R. & ANIKINA, E. (2003): Chromite composition and platinum-group mineral assemblage in the Uktus Uralian-Alaskan-type complex (Central Urals, Russia). *Mineral. Deposita* **38**, 312-326.

_____, ZACCARINI, F., CABELLA, R. & FERSHTATER, G. (1997b): Occurrence of unknown Ru–Os–Ir–Fe oxide in the chromitites of the Nurali ultramafic complex, southern Urals, Russia. *Can. Mineral.* **35**, 1431-1440.

_____, _____, _____, PUSHKAREV, E. & SMIRNOV,V. (1999c): Occurrence of platinum-group minerals in chromitites of the Kluchevskoy ophiolite complex,Central Urals, Russia: Preliminary results. *In* Mineral Deposits: Processes to Processing (C.J. Stanley *et al.*, eds.). A.A. Balkema, Rotterdam, The Netherlands (721-723).

_____, _____ & ECONOMOU-ELIOPOULOS, M. (1999a): Paragenesis and composition of laurite from chromitites of Othrys (Greece): implications for Os–Ru fractionation in ophiolitic upper mantle of the Balkan Peninsula. *Mineral. Deposita* **34**, 312-319.

_____, _____, MOLOSHAG, V. & ALIMOV, V. (1999b): Platinum-group minerals as indicator of sulfur fugacity in ophiolitic upper mantle: an example from chromitites of the Ray–Iz ultramafic complex (Polar Urals, Russia). *Can. Mineral*. **37**, 1099-1115.

GAUTHIER, M., CORRIVAUX, L., TROTTIER, L.J., CABRI, L.J., LAFLAMME, J.H.G. & BERGERON, M. (1990): Chromitites platinifères des complexes ophiolitiques de l'Estrie-Beauce, Appalaches du Sud du Québec. *Mineral. Deposita* **25**, 169-178.

GERVILLA, F. & LEBLANC, M. (1990): Magmatic ores in high-temperature Alpine-type lherzolite massifs (Ronda, Spain, and Beni Bousera, Morocco). *Econ. Geol*. **85**, 112-132.

KRAVCHENKO, G.G. (1986): Geological position and structure of chromite deposits in the Ural mountains. *In* Chromitites, UNESCO IGCP-197 project, Metallogeny of Ophiolites (W. Petrascheck *et al.*, eds). Theophrastus Publications, Athens, Greece (3-21).

LEBLANC, M., GERVILLA, F. & JEDWAB, J. (1990): Noble metals segregation and fractionation in magmatic ores from Ronda and Beni Busera lherzolite massifs (Spain, Morocco). *Mineral. Petrol*. **42,** 233-248.

_____ & NICOLAS, A. (1992): Ophiolitic chromitites. *Int. Geol. Rev.* **34**, 653-686.

MAIER, W.D., PRICHARD, H.M., FISHER, P.C. & BARNES, S.J. (1999): Compositional variation of laurite at Union Section in the western Bushveld Complex. *S. Afr. J. Geol.* **102**, 286-292.

MELCHER, F., GRUM, W., SIMON, G., THALHAMMER, T.V. & STUMPFL, E.F. (1997): Petrogenesis of the ophiolitic giant chromite deposits of Kempirsai, Kazakhstan: a study of solid and fluid inclusions in chromite. *J. Petrol.* **38**, 1419-1458.

_____, _____, THALHAMMER, T.V. & THALHAMMER, O.A.R. (1999): The giant chromite deposits at Kempirsai, Urals: constraints from trace element (PGE, REE) and isotope data. *Mineral. Deposita* **34**, 250-272.

MERKLE, R.K.W. (1992): Platinum-group minerals in the middle group of chromitite layers at Marikana, western Bushveld Complex: indications for collection mechanism and postmagmatic modification. *Can. J. Earth Sci.* **29**, 209-221.

MOLOSHAG, V.P. & SMIRNOV, S.V. (1996): Platinum mineralization of the Nurali mafic-ultramafic massif (Southern Urals). *Zap. Vses. Mineral. Obshchest.* **125**(1), 48-54 (in Russ.).

MUSSALLAM, K., JUNG, D. & BURGART, K. (1981): Textural features and chemical characteristics of chromites in ultramafic rocks, Chalkidiki complex (northeastern Greece). *Tschermaks Mineral. Petrogr. Mitt.* **29**, 75-101.

NALDRETT, A.J. & DUKE, J.M. (1980): Pt metals in magmatic sulfide ores. *Science* **208**, 1417-1424.

_____ & VON GRUENEWALDT, G. (1989): Association of platinum-group elements with chromitites in layered intrusions and ophiolite complexes. *Econ. Geol.* **84**, 180-187.

OHNENSTETTER, D., WATKINSON, D.H., JONES, P.C. & TALKINGTON, R. (1986): Cryptic compositional variation in laurite and enclosing chromite from the Bird River Sill, Manitoba. *Econ. Geol*. **81**, 1159-1168.

PERTSEV, A.N., SPADEA, P., SAVELIEVA, G.N. & GAGGERO, L. (1997): Nature of the transition zone in the Nurali ophiolite, southern Urals. *Tectonophys.* **276**, 163-180.

PROENZA, J., GERVILLA, F., MELGAREJO, J.C. & BODINIER, J.L. 1999. Al- and Cr-rich chromitites from the Mayarí–Baracoa Ophiolitic Belt (eastern Cuba): consequence of interaction between volatile-rich melts and peridotite in suprasubduction mantle. *Econ. Geol.* **94**, 547-566.

ROEDER, P.L. (1994): Chromite: from the fiery rain of chondrules to the Kilauea Iki lava lake. *Can. Mineral.* **32**, 729-746.

RUDNIK, G.B. (1965): Petrogenesis of ultramafic rocks of the Nurali massif in the South Urals. *In* Relationships of Magmatism and Metamorphism in the Genesis of Ultramafic Rocks. Nauka, Moscow, Russia (in Russ.; 68-100).

SAVELIEVA, G.N. (1987): *Gabbro-Ultrabasic Assemblages of the Uralian Ophiolites and their Analogues in Modern Oceanic Crust.* Nauka, Moscow, Russia (in Russ.).

_____ & SAVELIEV, A.A. (1992): Relationships between peridotites and gabbroic sequences in the ophiolites of the Urals and Lesser Caucasus. *Ofioliti* **17**, 117-138.

SMIRNOV, S.V. & VOLCHENKO, YU.A. (1992): The first finding of the platinum mineralization within chromite ore of the Nurali massif in the Southern Urals. *In* Yearbook 1991, Institute of Geology and Geochemistry, Ural Branch RAS, Ekaterinburg, Russia (115-117; in Russ.).

STOWE, C.W. (1994): Compositions and tectonic setting of chromite deposits through time. *Econ. Geol.* **89**, 528-546.

TALKINGTON, R.W. & LIPIN B.R. (1986): Platinum-group minerals in chromite seams of the Stillwater Complex, Montana. *Econ. Geol.* **81**, 1179-1186.

TORRES-RUIZ, J., GARUTI, G., GAZZOTTI, M., GERVILLA, F. & FENOLL HACH-ALÍ, P. (1996): Platinum-group minerals in chromitites from the Ojen lherzolite massif (Serrania de Ronda, Betic Cordillera, southern Spain). *Mineral. Petrol.* **56,** 25-50.

ZACCARINI, F., GARUTI, G. & CAWTHORN, G. (2002): Platinum-group minerals in chromitite xenoliths from the Onverwacht and Tweefontein ultramafic pipes, Eastern Bushveld Complex, South Africa. *Can. Mineral.* **40**, 481-497.

ZHOU, MEI-FU & BAI, WEN-JI (1992): Chromite deposits in China and their origin. *Mineral. Deposita* **27**, 192-199.

_____, MIN SUN, KEAYS, R.R. & KERRICH, R.W. (1998): Controls on platinum-group elemental distributions of podiform chromitites: a case study of high-Cr and high-Al chromitites from Chinese orogenic belt. *Geochim. Cosmochim. Acta* **62**, 677-688.

*Received December 15, 2002, revised manuscript accepted August 7, 2003.*